 doi:10.20944/preprints201708.0030.v1

Modeling NDVI using Joint entropy method considering hydro-meteorological driving factors in the middle reaches of Hei River basin

Zhang Gengxi[a], Xiaoling Su[a,*], Vijay P. Singh[b], Olusola O Ayantobo[a,c]

[a] College of Water Resources and Architectural Engineering, Northwest A & F University, Yangling 712100, China

[b] Department of Biological & Agricultural Engineering and Zachry Department of Civil Engineering, Texas A&M University, 2117 TAMU, College Station, TX 77843, USA

[c]Department of Water Resources Management and Agricultural-Meteorology, Federal University of Agriculture, PMB 2240, Abeokuta, Nigeria

*Corresponding author: College of Water Resources and Architectural Engineering, Northwest A and F University, Yangling 712100, China.

E-mail address: xiaolingsu@nwsuaf.edu.cn (X. Su)

 doi:10.20944/preprints201708.0030.v1

Abstract

Terrestrial vegetation dynamics are closely influenced by a multitude of factors. This study investigated the relationships between vegetation patterns and their main influencing factors. The joint entropy method was employed to evaluate the dependence between normalized difference vegetation index (NDVI) and coupled variables in the middle reaches of Hei River basin. Based on the spatial distribution of mutual information, the whole study area was divided into five sub-regions. In each sub-region, nested statistical models were applied to model the NDVI on the grid and regional scales, respectively. Results showed that the annual average NDVI increased with a rate of 0.005/a in recent 11 years. In the desert regions, the NDVI increased significantly with an increase in precipitation and temperature, and high accuracy of retrieving NDVI model was obtained by coupling precipitation and temperature, especially in sub-region I. In the oasis regions, groundwater was also an important factor driving vegetation growth, and the rise of groundwater level contributed to the growth of vegetation. However, the relationship was weaker in artificial oasis regions (sub-region III and sub-region V) due to the influence of human activities, such as irrigation. The overall correlation coefficient between the observed NDVI and modeled NDVI was observed to be 0.97. Outcomes of this study are suitable for ecosystem monitoring, especially under the realm of climate change. Further studies are necessary and should consider more factors, such as runoff and irrigation.

Key words: Joint entropy; NDVI; temperature; precipitation; groundwater depth; Hei River basin

 doi:10.20944/preprints201708.0030.v1

1. Introduction

Terrestrial vegetation plays a key role in energy, water, and biogeochemical cycles, while variation in vegetation can significantly influence the atmospheric processes. Vegetation is a sensitive indicator of global change and can also be a natural link between the atmosphere, land surface, soil, and water [1, 2]. The change in vegetation cover is influenced by climate change, human activities, and atmospheric CO_2 fertilization effect [3-5]. Evaluation of factors driving NDVI is important for analyzing the variability of vegetation.

Vegetation is strongly related to the amount and duration of precipitation and temperature, because they play a significant role in controlling vegetation development [2,6-8]. Several studies have reported relationships between vegetation indices and precipitation and temperature [3, 9-14]. However, most of these studies focused solely on either precipitation or temperature for vegetation models, thereby resulting in low precision and low correlation coefficients between vegetation indices and climatic variables [14]. For instance, Ichii et al. (2002) found a weaker relationship between vegetation growth and precipitation [15], while Nicholson et al. (1990) reported a weaker relationship between NDVI and precipitation, indicating a nonlinear overall relationship [16]. However, apart from the influence of climatic change, NDVI is also strongly related to the groundwater table level (GTL) in arid and semi-arid regions [2,17-19]. Many investigators have also reported the relationship between vegetation and groundwater availability (Lv et al., 2013; Jin et al., 2016). For instance, Jin et al. (2016) found a linear correlation between NDVI and groundwater depth in the Qaidam basin [2]. The distribution of GTL is becoming more heterogeneous in the middle reaches of Hei River as a result of increasing

 doi:10.20944/preprints201708.0030.v1

cultivated land area and runoff from Yingluo station [18]. The distribution of vegetation is also highly heterogeneous and depends on multiple factors. In this study, different statistical tools, as well as joint entropy method, were employed in order to understand the relationships between NDVI and precipitation, temperature, and GTL. This will be necessary for investigating the relevance of coupling variables.

Joint entropy expresses the total amount of uncertainty contained in the union of events [20] either in a linear or nonlinear system [21] and has been employed for various purposes. For instance, Li et al. (2012) employed joint entropy to design appropriate hydrometric networks, while Mishra et al. (2012) employed the entropy theory to overcome the nonlinear relationship between precipitation and vegetation, and further identified the downscaling method yielding higher mutual information [20]. Entropy theory has also been applied in ecological studies [14,22-24]. For instance, Phillips et al. (2006) modeled the geographic distribution of species using the maximum entropy. Sohoulande Djebou and Singh (2015) employed joint entropy to retrieve vegetation growth pattern from climatic variables. However, this study emphasizes mutual information of NDVI and the influencing factors.

In this paper, the mutual information of NDVI was investigated by coupling precipitation, temperature, and GTL. To that end, the study area was divided into 5 sub-regions, based on 3 spatial distributions of mutual information. In each subregion, NDVI was modeled using nested statistical models at the grid and regional scales, respectively.

2. Methodology

2.1Trend analysis

Preprints (www.preprints.org) | NOT PEER-REVIEWED | Posted: 8 August 2017 doi:10.20944/preprints201708.0030.v1

Trends for each pixel were represented to reflect the characteristics of vegetation cover in different periods of time [25]. The rate of change of NDVI was calculated as [26].

$$\theta_{slope} = \frac{n \times \sum_{i=1}^{n} i \times NDVI_i - \sum_{i=1}^{n} i \sum_{i=1}^{n} NDVI_i}{n \times \sum_{i=1}^{n} i^2 - (\sum_{i=1}^{n} i)^2} \quad (1)$$

where θ_{slope} is the slope of the trend line of annual NDVI; i represents the years; n is the time span; and $NDVI_i$ is the NDVI value for the ith year.

θ_{slope} describes the trend in the annual NDVI within the study area. If $\theta_{slope} > 0$, the NDVI increases; or else, the NDVI decreases ($\theta_{slope} < 0$) or remains constant($\theta_{slope} = 0$).

2.2 Joint entropy and mutual information

Mutual information was employed to explore the relationship between NDVI and influencing factors. Considering a random experiment X, for each value of X, x_i represents an event with a corresponding probability of occurrence, p_i. The entropy $H(X)$ can be expressed as:

$$H(X) = -\sum_{i=1}^{n} p_i \log_2(p_i) \quad (2)$$

The logarithm is based on 2, because it is more convenient to use logarithms than base e or 10, however, the base can be taken as other than 2 without alteration [21]. The entropy is thereby measured in bits. The Probability Density Function (PDF) of variable X is obtained using discrete intervals for the values of X. The discrete PDF is defined for n equal-width bins defined for the range of X [14,21,27]. The entropy $H(X)$

Preprints (www.preprints.org) | NOT PEER-REVIEWED | Posted: 8 August 2017 doi:10.20944/preprints201708.0030.v1

is a measurement of information or uncertainty [21]. Similarly, the joint entropy can be computed for a joint probability distribution of two or more variables [21,28]. Specifically, with three variables, the joint PDF is computed based on a three-dimensional contingency analysis as illustrated in Table 1. Considering the three variables: precipitation, temperature and NDVI, the process generates a discrete PDF made of n^3 discrete probabilities such that:

$$\sum_{i=1}^{n}\sum_{j=1}^{n}\sum_{k=1}^{n} p(P=P_i, T=T_i, NDVI=NDVI_i)=1 \quad (3)$$

The joint entropy of the three variables can be defined as：

$$H(P,T,NDVI)=-\sum_{i=1}^{n}\sum_{j=1}^{n}\sum_{k=1}^{n} p(P_i,T_j,NDVI_k)\log_2[p(P_i,T_j,NDVI_k)] \quad (4)$$

Table1.....

The mutual information represents the amount of information common to both X and Y and provides a general measure of dependence between the random variables. It is superior to the Pearson correlation coefficient, because it captures both linear and nonlinear dependence while the Pearson correlation coefficient is only suitable for linear relationships [28]. It equals the difference between the sum of two marginal entropies and the total entropy:

$$M(X,Y)=H(X)+H(Y)-H(X,Y) \quad (5)$$

The two-dimensional cases of the amount of information transmitted can be extended to three or more dimensional cases [29]. Considering three variables of precipitation, temperature, and NDVI, precipitation and temperature are considered as inputs while NDVI an output. Therefore:

Preprints (www.preprints.org) | NOT PEER-REVIEWED | Posted: 8 August 2017 doi:10.20944/preprints201708.0030.v1

$$M(P,T;NDVI) = H(P,T) + H(NDVI) - H(P,T,NDVI) \quad (6)$$

Moreover, applying the same methodology, the coupling of *P* and GTL; *T* and *GTL* along with NDVI were further explored. The ensemble *E* of candidate equations can be summarized as:

$$E = \{NDVI_{GTL,P} = f(GTL,P); NDVI_{GTL,T} = f(GTL,T); NDVI_{T,P} = f(T,P)\} \quad (7)$$

3. Study area and data

The study area occupied the middle reaches of the Hei River basin (38°30′-39°55′N, 98°55′-100°55′E; Fig. 1), which is located in the middle of Hexi corridor of Gansu Province, northwest of China, and belongs to an arid climate zone. The total area is about 10000 km^2. The mean annual temperature is around $8°C$, and mean annual precipitation is between 69 and 216 mm and is concentrated between June and September, while the mean annual potential evaporation is between 1453 and 2351 mm [30].

Fig. 1. .....

The Hei River is the second largest inland river in China with a total length of 821 km and a runoff of 16.0×10^8 m^{3}yr^{-1}. It flows through Yingluoxia and Zhengyixia station entering and exiting middle reaches. Runoff has shown an increasing/decreasing trend in the past decade. The annual runoff at Yingluoxai station increased to 16.0×10^8m^3 in the 1990s from around 14.4×10^8m^3 in the 1960s(Fig. 2), while the runoff at Zhengyixai station decreased by 3×10^8m^3 during the same time period (Fig. 2). This situation accelerated desertification within the northern parts of

Preprints (www.preprints.org) | NOT PEER-REVIEWED | Posted: 8 August 2017 doi:10.20944/preprints201708.0030.v1

the basin [31,32]. In order to mitigate deteriorating ecosystems in the Hei River basin, an Ecological Water Diversion Project (EWDP) was initiated by the Chinese government in 2000 to ensure the delivery of water to the lower reaches for ecological water needs [33]. After that, runoff at Zhengyixia station has increased to levels not recorded since the 1960s [31,34]. The implementation of EWDP alleviated the ecological deterioration in the lower reaches of Hei River but aggravated the water resources shortage in the middle reaches. In order to meet the increasing demand for water resources, groundwater exploration provided an option. After 2004, the recharge of groundwater also increased due to the increase in precipitation, irrigation and runoff replenishment. The temporal variation in groundwater levels of the observation wells during 2001 to 2011 is shown in Fig.3(c) which shows a rising trend in groundwater level along the Heihe River [35]. However, the water level in the region away from the river showed a declining trend.

Fig. 2.....

The annual NDVI of each pixel was calculated by the annual maximum value of NDVI in order to eliminate the noise from the cloud and solar altitude. The NDVI datasets were acquired from National Natural Science Foundation of China "Environmental and Ecological Science Data Center in the West of China (http://westdc.westgis.ac.cn/)" with a spatial resolution of 1 km and temporal resolution of 1 day, groundwater depths of 53 wells were obtained from National Natural Science Foundation of China "Hei River Project Data Management Center (http://www.heihedata.org/)" while monthly precipitation and temperature datasets were acquired from China Meteorological Network (http://data.cma.cn/), with a 0.5°

Preprints (www.preprints.org) | NOT PEER-REVIEWED | Posted: 8 August 2017 doi:10.20944/preprints201708.0030.v1

spatial resolution.

The ordinary kriging method was employed to interpolate the observed values of ground water depths. For consistency regarding the NDVI spatial resolution, the interpolated groundwater table levels, precipitation, and temperature datasets were rescaled to a 1 km spatial resolution.

Fig. 3. .....

Fig. 4. .....

4. Results and discussion

4.1 Variation of Hydrometeorological variables and NDVI

During the period of 2001-2011, both the average temperature and cumulative precipitation increased at the three hydrologic stations (Fig. 3 (a,b)). The distributions of cumulative precipitation and average temperature are shown in Fig. 4 (a,b). Temperature gradually rises from south to north, while precipitation decreases were also observed. This is mainly determined by topography.

Fig. 5 (a) illustrates the annual maximum NDVI in the middle reaches of Hei River basin from 2000 to 2011. The slope of the linear regression trend-line was 0.005. The NDVI time series corresponded to the average of all the pixels in the study area and reflected the overall trend. Fig.5 (b) shows the spatial distribution of the linear regression slope (θ_{slope}). In most cases, the area, where NDVI increased, occupied about 94% of the total area.

Fig. 5. .....

 doi:10.20944/preprints201708.0030.v1

3.2 Mutual information of NDVI with coupling of variables

To understand the relationship between NDVI and hydro-meteorological variables, mutual information was employed to measure the dependence between the NDVI time series and each coupled variable. The greater the values of mutual information the higher the correlation. The spatial distribution of mutual information between NDVI and coupled variables are shown in Figures 6 (a), (b), and (c), respectively. It can be observed from the figures that the mutual information of NDVI and coupled variables of precipitation and GTL generally decreased from southeast to northwest. The mutual information values of NDVI and coupled variables of precipitation and temperature were dispersedly distributed, increasing from the center to the edge of regions, while the mutual information of NDVI and coupled variables of temperature and groundwater table levels was greater in the northwestern and southeastern regions. In order to appropriately model the NDVI using dependent variables, the study region was divided into 5 sub-regions, based on three spatial distributions of mutual information (Fig 6(d)).

In sub-regions I and IV, precipitation and temperature were used to model the NDVI, since the mutual information of NDVI and variables of precipitation and temperature were relatively higher. GTL and precipitation were used to model the NDVI in sub-regions II and V, while temperature and GTL were selected to model the NDVI in sub-region III.

Fig. 6. .....

 doi:10.20944/preprints201708.0030.v1

4.3 Modelling NDVI

Nested statistical models were developed for modeling NDVI in each subregion. In most cases, the linear fitting of NDVI time series to precipitation, temperature, and GTL resulted in poor correlation coefficients and high root means square error [14]. The vegetation growth may not be monotonic in relation to the atmospheric variables. For example, the temperature sensitivity of photosynthesis increases up to an optimum and later decreases as temperature gets higher [14]. A two-dimensional fitting was used to model NDVI using each of the hydrometeorological variables as a factor. It was discovered that a logarithmic transformation of precipitation gave a better correlation with NDVI in some sub-regions. Considering GTL and temperature, a negative exponential and a quadratic model showed a better relationship with NDVI. However, a linear regression model exhibited a better relationship between temperature and NDVI in sub-region I.

Different candidate equations were used to fit NDVI by coupling pair-wise precipitation, temperature, and GTL. The aim of the fitting procedures was to maximize the correlation coefficient and minimize the sum of squared residuals. However, the main importance of the fitting procedure was to maximize the proportion of the area in which the correlation coefficient met with significance testing.

 doi:10.20944/preprints201708.0030.v1

Table 2.....

In each sub-region, analysis was performed at the grid scale. In sub-regions I and IV, the coupling of precipitation and temperature resulted in a model of NDVI time series with an average correlation coefficient of 0.68 and 0.58, respectively. However, the percentage of area in which the correlation coefficient met with significance testing was only 42% in sub-region IV. This was mainly because the temperature was relatively high, thereby increasing evapotranspiration and water demand for vegetation growth that precipitation was unable to satisfy. In sub-regions II and V, the best fitting models were obtained by combing pair-wise negative exponentially transformed GTL respectively with the logarithmically and linearly transformed precipitation. In sub-region V, the percentage area in which the correlation coefficient met with the significance testing was only 44%. There was a large area of arable land and artificial grassland in sub-region V (Fig. 1). In sub-regions III and V, the growth of vegetation was strongly influenced by human activities, e.g. irrigation. Therefore, irrigation was the main influencing factor for vegetation growth. Beyond that, there was a considerable amount of water in sub-region III, thereby influencing the prediction accuracy. After various fittings in different sub-regions, the correlation coefficients were combined for the entire study area (Fig. 7). Results showed that there was about 52% area in which the correlation coefficients met with significance testing.

Fig.7.....

Analysis was also performed at a regional scale. Using the average NDVI time

Preprints (www.preprints.org) | NOT PEER-REVIEWED | Posted: 8 August 2017 doi:10.20944/preprints201708.0030.v1

series of different sub-regions as predicted and each of the average hydro-meteorological variables as predictor, a two-dimensional fitting was employed in the five sub-regions, respectively. This prediction also employed the same formulas used for the prediction at a grid scale (table 2). Figures 8(a-e) showed the results of the three-dimensional scatter-plot couplings. Comparison of this figure showed that sub-regions I and II had a better accuracy of fitting. Figures 8(f) presents the overall relationship between observed NDVI and modeled NDVI for the whole region, where the correlation coefficient was observed to be 0.97, which indicated a high accuracy. This showed that this method was suitable for NDVI modeling.

4. Conclusions

In this study, the spatiotemporal variation of vegetation cover in the middle reaches of Hei River basin and the main driving factors during the period of 2001-2011 were analyzed using MODIS NDVI data and hydro-meteorological data. Considering the nonlinear relationship between hydro-meteorological variables, the entropy theory was employed to calculate the mutual information between NDVI time series and coupled hydro meteorological variables. Based on the spatial distribution of mutual information, the whole region was further divided into 5 sub-regions, and nested statistical models were employed to simulate NDVI in each sub-region. The main conclusions are as follows:

(1)The average annual NDVI increased at a rate of 0.005/a in recent 11 years in the middle reaches of Hei River. The percentage area where NDVI increased occupied

 doi:10.20944/preprints201708.0030.v1

94% of the total area.

(2) In the desert sub-regions (I and IV), temperature and precipitation are the main driving factors for vegetation growth. The increase in precipitation and temperature obviously led to a significant increase in NDVI. However, in the oasis regions (sub-region II and sub-region III), groundwater was an important factor for vegetation growth.

(3) In coupling hydro meteorological variables, a nested statistical model was proposed for modeling NDVI on a regional scale. The overall correlation coefficient between observed NDVI and modeled NDVI was observed to be 0.97. This high simulation accuracy further proves the suitability of this method.

(4) Due to the influence of human activities, the modeling accuracy was not effective within the artificial oasis (sub-region III and sub-region V). Therefore, further studies are necessary for modeling NDVI, considering more factors such as runoff and irrigation using long-term data sets.

Supplementary Materials:

Preprints (www.preprints.org) | NOT PEER-REVIEWED | Posted: 8 August 2017 doi:10.20944/preprints201708.0030.v1

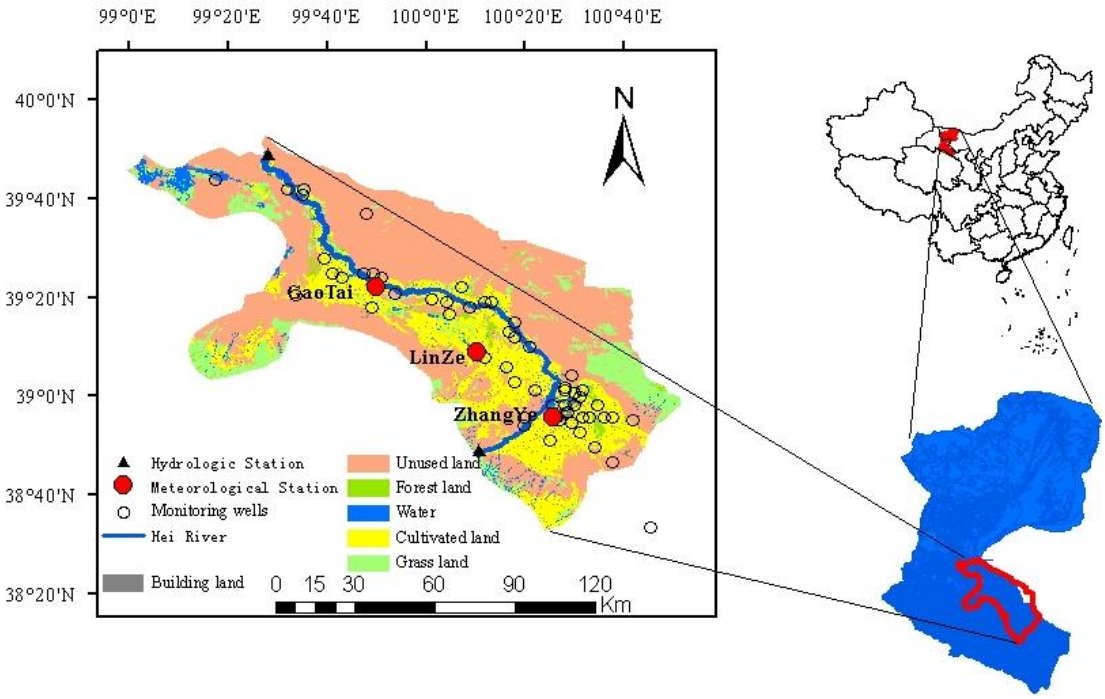

Fig.1. Map of the middle reaches of Hei River basin and the monitoring wells

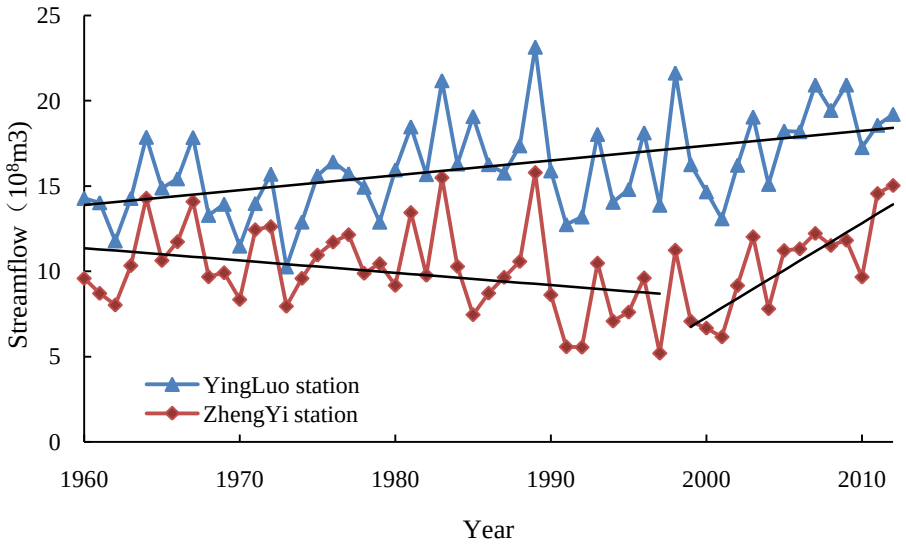

Fig.2.Annual discharge of Heihe River at Yinluoxia and Zhengyixia stations

Preprints (www.preprints.org) | NOT PEER-REVIEWED | Posted: 8 August 2017 doi:10.20944/preprints201708.0030.v1

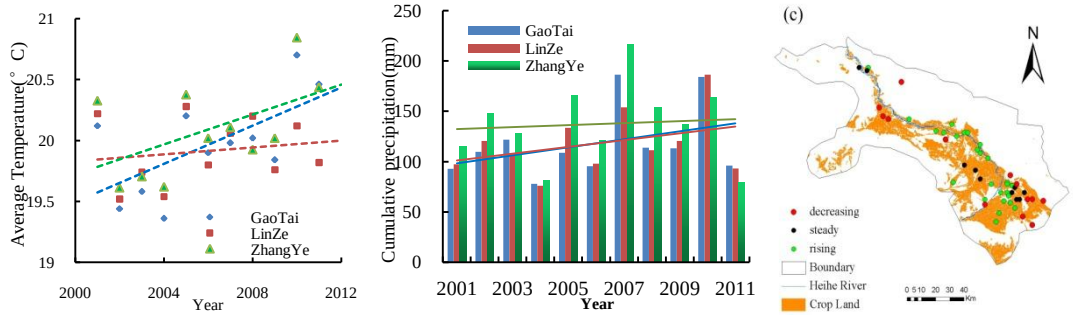

Fig.3. The temporal variation of average temperature(a), cumulative precipitation(b) and average ground depths(c)

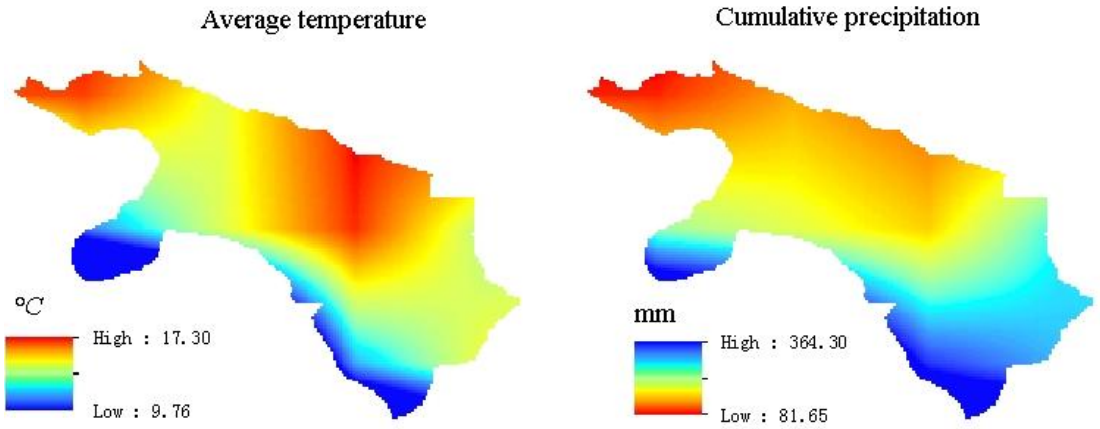

Fig.4. The spatial distribution of (a) average temperature, (b) cumulative precipitation

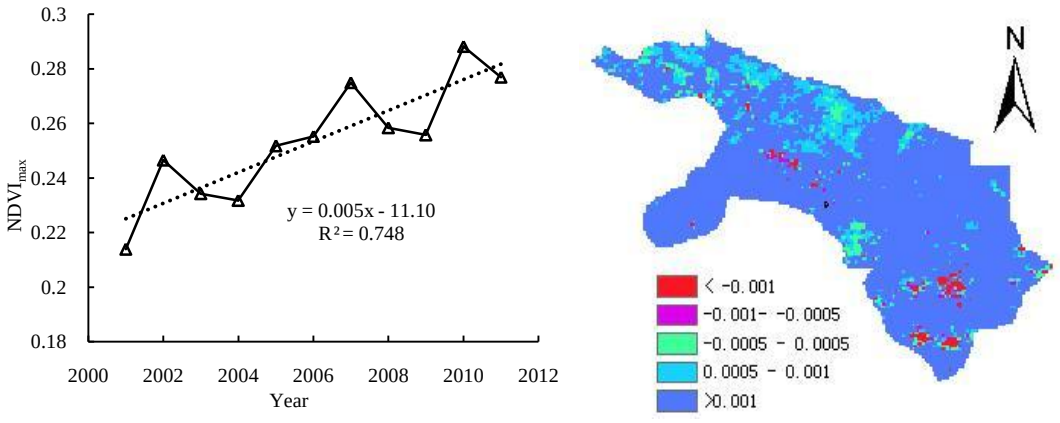

Fig.5. Inter-annual variability of annual NDVI (a) and the trends of NDVI (b)

Preprints (www.preprints.org) | NOT PEER-REVIEWED | Posted: 8 August 2017 doi:10.20944/preprints201708.0030.v1

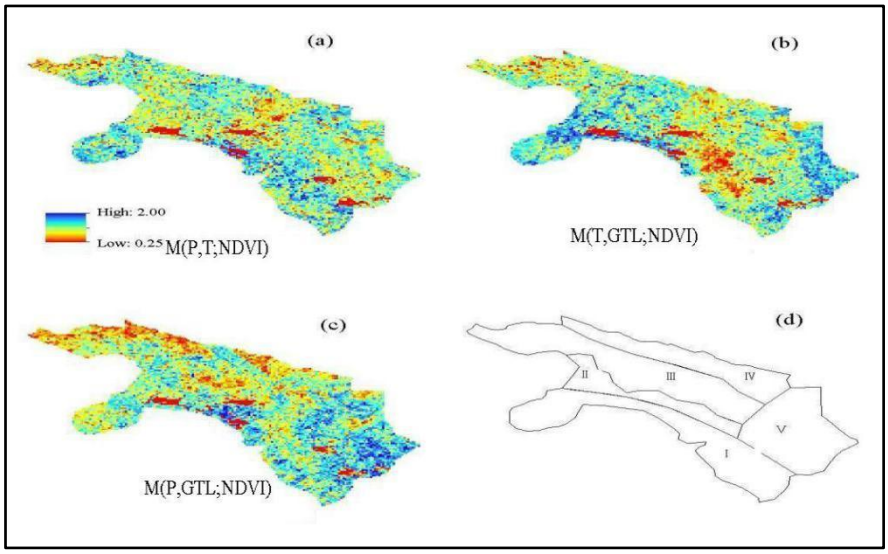

Fig.6. The distribution of mutual information of NDVI and three coupling hydro-meteorological variables(a)-(c) and the divided sub-regions(d)

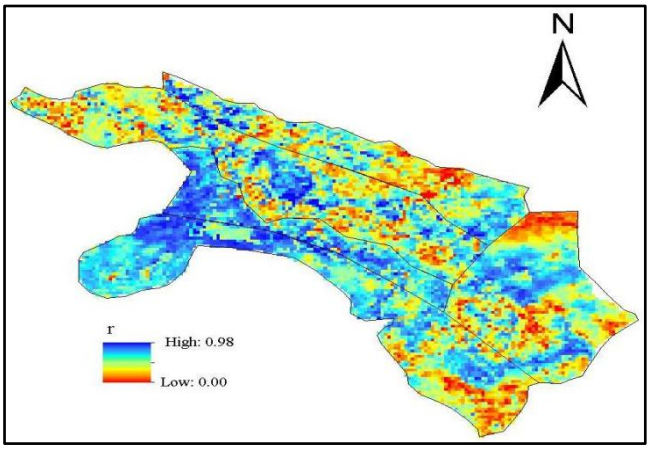

Fig.7. The distribution of correlation coefficients of estimated NDVI by coupling hydro-meteorological variables

Preprints (www.preprints.org) | NOT PEER-REVIEWED | Posted: 8 August 2017 doi:10.20944/preprints201708.0030.v1

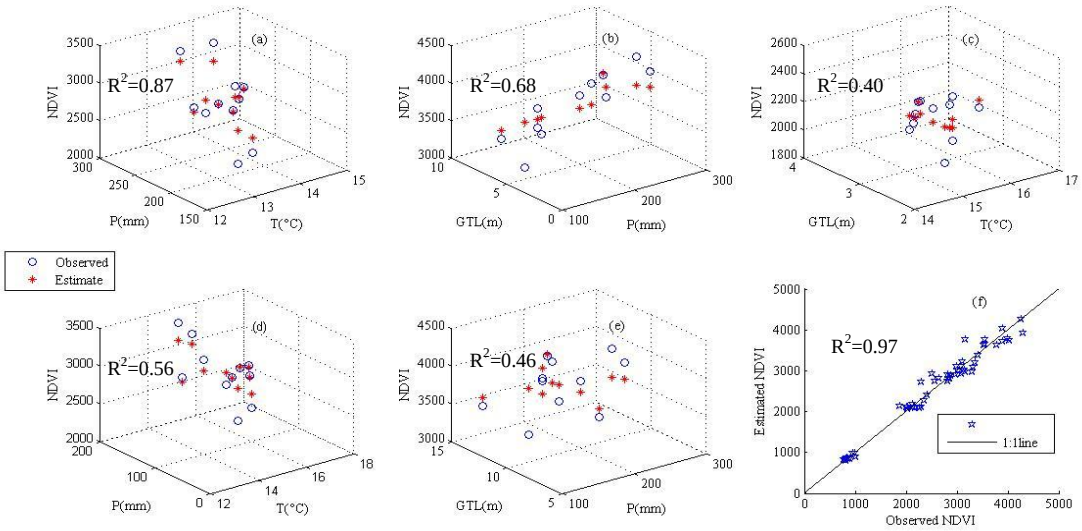

Fig.8. Three dimensional scatter plots of NDVI (multiplied by 10^4) in five sub-regions (a-e) and the relationship between observed NDVI modeled NDVI in the whole region(f).

Table1 Illustration of a three-dimension contingency employed to compute the joint PDF. Consider 3 variables *X*, *Y*, and *Z*.

Variables			Discrete probabilities
$X=\{X_1,X_2\}$	$Y=\{Y_1,Y_2\}$	$Z=\{Z_1,Z_2\}$	
$X=X_1$	$Y=Y_1$	$Z=Z_1$	$p(X=X_1,Y=Y_1,Z=Z_1)$
		$Z=Z_2$	$p(X=X_1,Y=Y_1,Z=Z_2)$
	$Y=Y_2$	$Z=Z_1$	$p(X=X_1,Y=Y_2,Z=Z_1)$
		$Z=Z_2$	$p(X=X_1,Y=Y_2,Z=Z_2)$
$X=X_2$	$Y=Y_1$	$Z=Z_1$	$p(X=X_2,Y=Y_1,Z=Z_1)$

Preprints (www.preprints.org) | NOT PEER-REVIEWED | Posted: 8 August 2017 doi:10.20944/preprints201708.0030.v1

		$Z=Z_2$	$p(X=X_2,Y=Y_1,Z=Z_2)$
	$Y=Y_2$	$Z=Z_1$	$p(X=X_2,Y=Y_2,Z=Z_1)$
		$Z=Z_2$	$p(X=X_2,Y=Y_2,Z=Z_2)$

Note: Each variable is categorized into 2 classes(n=2)

Table 2. Fitting models, correlation coefficients and area proportion meeting significance testing in five subregions

Subregion No.	Fitting formula	Average correlation coefficient	Areaproportion ($p<0.05$)
I	$NDVI_{T,P}=a\ln(P+b)+cT^2+d\cdot T+e$	0.68	0.75
II	$VI_{GTL,P}=a\cdot e^{-(GTL+b)}+c\cdot\ln(P+d)$	0.66	0.72
III	$VI_{GTL,T}=a\cdot GTL+b\cdot T^2+c\cdot T+d$	0.43	0.34
IV	$VI_{T,P}=a\cdot P+b\cdot T^2+c\cdot T+d$	0.58	0.42
V	$VI_{GTL,P}=a\cdot e^{-(GTL+b)}+c\cdot P+d$	0.53	0.44

Acknowledgments: We are grateful for the grant support from the National Natural Science Fund in China (91425302 and 51279166).

Authors Contributions: Gengxi Zhang and Xiaoling Su designed the computations and wrote the paper; Vijay P. Singh and Olusola O Ayantobo revised the paper and gave some suggestions; All authors have read and approved the final manuscript.

Conflicts of Interest: The authors declare no conflict of interest.

Reference:

1. Kutiel, P.;Cohen, O.;Shoshany, M.;Shub, M. Vegetation establishment on the southern Israeli coastal sand dunes between the years 1965 and 1999. *Landscape and Urban Planning*, **2004**, 67: 141-156.doi:10.1016/s0169-2046(03)00035-5
2. Jin, X.;Liu, J.;Wang, S.;Xia, W. Vegetation dynamics and their response to groundwater and climate variables in Qaidam Basin, China. *International Journal of Remote Sensing*, **2016**, 37: 710-728.doi:10.1080/01431161.2015.1137648
3. Piao, S.;Mohammat, A.;Fang, J.;Cai, Q.;Feng, J. NDVI-based increase in growth of temperate grasslands and its responses to climate changes in China. *Global Environmental Change*, **2006**, 16: 340-348.doi:10.1016/j.gloenvcha.2006.02.002
4. Dai, S.;Zhang, B.;HaiJun, W.;YaMin, W.;LingXia, G.;XingMei, W.;Dan, L. I. Vegetation cover change and the driving factors over northwest China. *Journal of Arid Land*, **2011**, 3: 25-33.doi:10.3724/sp.j.1227.2011.00025
5. Liu, J.;Wu, J.;Wu, Z.;Liu, M. Response of NDVI dynamics to precipitation in the Beijing–Tianjin sandstorm source region. *International Journal of Remote Sensing*, **2013**, 34: 5331-5350.doi:10.1080/01431161.2013.787505
6. Clerici, N.;Weissteiner, C. J.;Gerard, F. Exploring the Use of MODIS NDVI-Based Phenology Indicators for Classifying Forest General Habitat Categories. *Remote Sensing*, **2012**, 4: 1781-1803.doi:10.3390/rs4061781
7. Feilhauer, H.;He, K. S.;Rocchini, D. Modeling Species Distribution Using Niche-Based Proxies Derived from Composite Bioclimatic Variables and MODIS NDVI. *Remote Sensing*, **2012**, 4: 2057-2075.doi:10.3390/rs4072057
8. Rousvel, S.;Armand, N.;Andre, L.;Tengeleng, S. Comparison between vegetation and rainfall of Bioclimatic Ecoregions in Central Africa. *Atmosphere*, **2013**: 411-427.doi:10.3390/atmos4040411
9. Brunsell, N. A.;Young, C. B. Land surface response to precipitation events using MODIS and NEXRAD data. *International Journal of Remote Sensing*, **2008**, 29: 1965-1982.doi:10.1080/01431160701373747
10. Kawabata, A.;Ichii, K.;Yamaguchi, Y. Global monitoring of interannual changes in vegetation activities using NDVI and its relationships to temperature and precipitation. *International Journal of Remote Sensing*, **2001**, 22: 1377-1382.doi:10.1080/01431160119381
11. Pettorelli, N.;Pelletier, F.;von Hardenberg, A.;Festa-Bianchet, M.;Cote, S. D. Early onset of vegetation growth vs. rapid green-up: Impacts on juvenile mountain ungulates. *Ecology*, **2007**, 88: 381-390.doi:10.1890/06-0875
12. Piao, S.;Nan, H.;Huntingford, C.;Ciais, P. Evidence for a weakening relationship between interannual temperature variability and northern vegetation activity. *Nature Communications*, **2014**, 510.doi:10.1038/ncomms6018
13. Pielke, R. A.;Avissar, R. Interactions between the atmosphere and terrestrial ecosystems: influence on weather and climate. *Global change biology*, **1998**: 461-475. doi:50 53c165e4 b097cd4fcef83c
14. Sohoulande Djebou, D. C.;Singh, V. P. Retrieving vegetation growth patterns from soil moisture, precipitation and temperature using maximum entropy. *Ecological Modelling*, **2015**, 309-310: 10-21.doi:10.1016/j.ecolmodel.2015.03.022

15. Ichii, K.;Kawabata, A.;Yamaguchi, Y. Global correlation analysis for NDVI and climatic variables and NDVI trends: 1982-1990. *International Journal of Remote Sensing*, **2002**, 23: 3873-3878.doi:10.1080/01431160110119416
16. Nicholson, S. E.;Davenport, M. L.;Mao, A. R. A comparison of the vegetation response to rainfall in the Sahel and East-Africa, using normalized difference vegetation index from NOAA AVHRR. *Climate Change*, **1990**, 17: 209-241.
17. Jin, X. M.;Guo, R. H.;Zhang, Q.;Zhou, Y. X.;Zhang, D. R.;Yang, Z. Response of vegetation pattern to different landform and water-table depth in Hailiutu River basin, Northwestern China. *Environmental Earth Sciences*, **2014**, 71: 4889-4898.doi:10.1007/s12665-013-2882-1
18. Lv, J.;Wang, X.-S.;Zhou, Y.;Qian, K.;Wan, L.;Eamus, D.;Tao, Z. Groundwater-dependent distribution of vegetation in Hailiutu River catchment, a semi-arid region in China. *Ecohydrology*, **2013**, 6: 142-149.doi:10.1002/eco.1254
19. Jin, X. M.;Schaepman, M. E.;Clevers, J.;Su, Z. B.;Hu, G. C. Groundwater Depth and Vegetation in the Ejina Area, China. *Arid Land Res. Manag.*, **2011**, 25: 194-199.doi:10.1080/15324982.2011.554953
20. Mishra, A. K.;Ines, A. V. M.;Singh, V. P.;Hansen, J. W. Extraction of information content from stochastic disaggregation and bias corrected downscaled precipitation variables for crop simulation. *Stochastic Environmental Research and Risk Assessment*, **2012**, 27: 449-457.doi:10.1007/s00477-012-0667-9
21. Singh, V. P. Entropy theory and its application in environmental and water engineering; John Wiley & Sons: New York, NY, USA, 2013.
22. Phillips, S. J.;Anderson, R. P.;Schapire, R. E. Maximum entropy modeling of species geographic distributions. Ecological Modelling, 2006, 190: 231-259. doi:10.1016/j.eco lmodel. 2005.03.026
23. Pueyo, S.;He, F.;Zillio, T. The maximum entropy formalism and the idiosyncratic theory of biodiversity. *Ecology Letters*, **2007**, 10: 1017-1028.doi:10.1111/j.1461-0248.2007.01096.x
24. Urbani, F.;D'Alessandro, P.;Frasca, R.;Biondi, M. Maximum entropy modeling of geographic distributions of the flea beetle species endemic in Italy (Coleoptera: Chrysomelidae: Galerucinae: Alticini). *Zoologischer Anzeiger - A Journal of Comparative Zoology*, **2015**, 258: 99-109.doi:10.1016/j.jcz.2015.08.002
25. Liu, J.;Wu, J.;Wu, Z.;Liu, M. Response of NDVI dynamics to precipitation in the Beijing-Tianjin sandstorm source region. *International Journal of Remote Sensing*, **2013**, 34: 5331-5350.doi:10.1080/01431161.2013.787505
26. Song, Y.;Ma, M. Varition of AVHRR NDVI and its relationship with climate in Chinese arid and cold regions. *Journal of Remote sensing*, **2008**, 12: 499-505.
27. Sohoulande Djebou, D. C.;Singh, V. P.;Frauenfeld, O. W. Analysis of watershed topography effects on summer precipitation variability in the southwestern United States. *Journal of Hydrology*, **2014**, 511: 838-849.doi:10.1016/j.jhydrol.2014.02.045
28. Li, C.;Singh, V. P.;Mishra, A. K. Entropy theory-based criterion for hydrometric network evaluation and design: Maximum information minimum redundancy. *Water Resources Research*, **2012**, doi:4810.1029/2011wr011251
29. McGill, W. J. Mutivariate information transmisson. *Psychometrica*, **1954**, 19: 97-116.
30. Nian, Y.;Li, X.;Zhou, J.;Hu, X. Impact of land use change on water resource allocation in the middle reaches of the Heihe River Basin in northwestern China. *Journal of Arid Land*, **2013**, 6:

273-286.doi:10.1007/s40333-013-0209-4

31. Wang, Y.;Roderick, M. L.;Shen, Y.;Sun, F. Attribution of satellite-observed vegetation trends in a hyper-arid region of the Heihe River basin, Western China. *Hydrology and Earth System Sciences*, **2014**, 18: 3499-3509.doi:10.5194/hess-18-3499-2014
32. Guo, Q.;Feng, Q.;Li, J. Environmental changes after ecological water conveyance in the lower reaches of Heihe River, northwest China. *Environmental Geology*, **2008**, doi:5810.1007/s00254-008-1641-1
33. Zhang, A.;Zheng, C.;Wang, S.;Yao, Y. Analysis of streamflow variations in the Heihe River Basin, northwest China: Trends, abrupt changes, driving factors and ecological influences. *Journal of Hydrology: Regional Studies*, **2015**, 3: 106-124.doi:10.1016/j.ejrh.2014.10.005
34. Qin, D.;Zhao, Z.;Han, L.;Qian, Y. Determinnation of groundwater recharge regim and flowpath in the Lower Heihe River basin in an arid area of Northwest China by using environmental tracers: Implications for vegetation degradation in the Ejina Oasis. *Applied Geochemistry*, **2012**: 1133-1145.doi:10.1016/j.apgeachem.2012.02.031
35. Mi, L.;Xiao, H.;Zhang, J.;Yin, Z.;Shen, Y. Evolution of the groundwater system under the impacts of human activities in middle reaches of Heihe River Basin (Northwest China) from 1985 to 2013. *Hydrogeology Journal*, **2016**, 24: 971-986.doi:10.1007/s10040-015-1346-y